JOURNAL OF VIROLOGY, Aug. 1992, p. 5075–5086
0022-538X/92/085075-12$02.00/0

Vol. 66, No. 8

# Linker Scanning Mutagenesis of the Internal Ribosome Entry Site of Poliovirus RNA

AURELIA A. HALLER AND BERT L. SEMLER*

*Department of Microbiology and Molecular Genetics, College of Medicine, University of California, Irvine, California 92717-4025*

Received 1 April 1992/Accepted 19 May 1992

**The initiation of cap-independent translation of poliovirus mRNA occurs as a result of ribosome entry at an internal site(s) within the 5′ noncoding region. A series of linker scanning mutations was constructed to define the genetic determinants of RNA-protein interactions that lead to high-fidelity translation of this unusual viral mRNA. The mutations are located within two distinct stem-loop structures in the 5′ noncoding region of poliovirus RNA that constitute a major portion of a putative internal ribosome entry site. On the basis of our data derived from genetic and biochemical assays, the stability of one of the stem-loop structures appears to be essential for translation initiation via internal binding of ribosomes. However, the second stem-loop structure may function in a manner that requires base pairing and proper spacing between specific nucleotide sequences. By employing RNA electrophoretic mobility shift assays, an RNA-protein interaction was detected for this latter stem-loop structure that does not occur in RNAs containing mutations which perturb the predicted hairpin structure. Analysis of in vivo-selected virus revertants, in combination with mobility shift assays, suggests that extensive genetic rearrangement can lead to restoration of 5′ noncoding region functions, possibly by the repositioning of specific RNA sequence or structure motifs.**

The following three features define a eukaryotic mRNA as an efficient template for translation initiation: (i) a 5′ 7-methylguanosine cap structure which facilitates recognition and binding of the 43S ternary ribosomal subunit, (ii) a single AUG in a favorable sequence context in which translation initiates, and (iii) a lack of secondary structure in the 5′ untranslated region which appears to promote scanning of the mRNA by the 40S ribosomal subunit. Translation initiation of most eukaryotic mRNAs occurs via a mechanism that is consistent with the ribosome scanning model (21). The introduction of a stable hairpin in the 5′ untranslated region of a eukaryotic mRNA decreases the efficiency of translation of such an mRNA template as a result of the inability of the scanning ribosome to melt stable secondary structures (40). However, some cellular and viral mRNAs contain structural or sequence-specific features at the 5′ ends of their mRNAs that would be predicted to impair translation initiation. For example, the 5′ untranslated region (also called noncoding region [NCR]) of the *BCR/ABL* oncogene mRNA contains multiple upstream AUGs in a favorable context (34), and a stable secondary structure in the 5′ NCR of the rat ornithine decarboxylase mRNA is predicted from the nucleotide sequence (29), both of which would predictably delay or stop scanning ribosomes. Recently, a cellular mRNA encoding the immunoglobulin heavy-chain-binding protein (Bip) which is capable of internal translation initiation was identified. Translation of this cellular mRNA continues even during a poliovirus infection that results in the shutoff of cap-dependent protein synthesis (28). Indeed, the translation of poliovirus RNA occurs via a mechanism that does not require the three RNA sequence and/or structure requirements described above.

Poliovirus, like all members of the *Picornaviridae* family (e.g., coxsackievirus, human rhinovirus, encephalomyocarditis virus [EMCV], and foot-and-mouth disease virus), has a long (~750 nucleotides [nt]) 5′ NCR that contains unusual features which will not accommodate the RNA-protein dynamics implicated in the scanning model for translation initiation. These features are present in the 5′ NCR of a single-stranded, message sense, genomic RNA of ~7.5 kb in length. The 742-nt-long 5′ NCR precedes a polyprotein-coding region and contains an extensive secondary structure and multiple AUGs upstream of the translation initiation site. In addition, the 5′ end of poliovirus mRNA lacks a 7-methylguanosine cap structure. Rather, it contains a pUp structure that is produced following removal of a 22-amino-acid genome-linked protein (VPg) from genomic RNA that associates with polyribosomes (37).

Collectively, the data above predict that sequences within the 5′ NCR of picornavirus RNAs contain signals and/or structures that facilitate cap-independent initiation of translation. For the viral mRNAs of poliovirus (41), EMCV (14, 15, 18), and foot-and-mouth disease virus (1, 23), convincing evidence which suggests that the mechanism of cap-independent translation initiation involves internal ribosome entry has been presented. The poliovirus RNA sequences critical for cap-independent translation were mapped to nt 320 to 630 of the 5′ NCR (39). Another study defined the region important for viral protein synthesis to be located between nt 560 and 627 (2). Within the region of the poliovirus genome involved in translation initiation are nucleotide sequences harboring some interesting features. A polypyrimidine tract, beginning at nt 558, and an AUG located at nt 586 are highly conserved among the enteroviruses (e.g., poliovirus and coxsackievirus) and the rhinoviruses (Fig. 1). This AUG is part of a conserved octamer. The region containing the polypyrimidine tract is shown as a single-stranded region in the diagram in Fig. 1, as predicted by some investigators (46), but for the purpose of this study, we will adhere to computer predictions (confirmed by nuclease treatment studies) that show base pairing of a portion of the polypyrimidine tract (43). The region of the poliovirus 5′ NCR that appears to be involved in the internal binding of ribosomal

* Corresponding author.

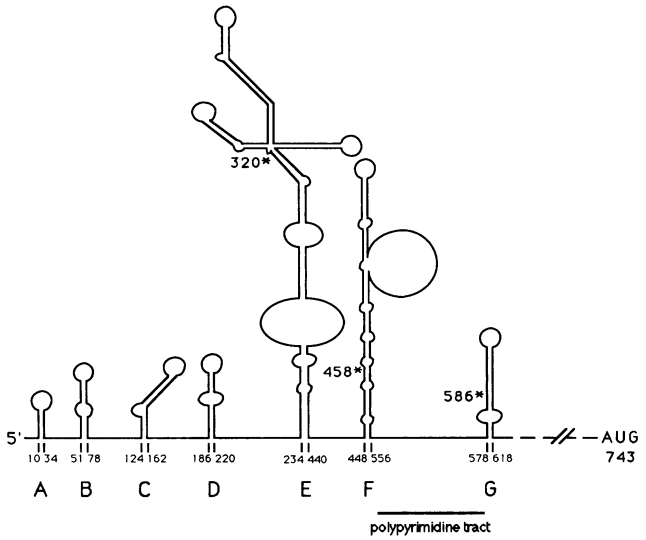


FIG. 1. A diagram of the computer-predicted secondary structure of the 5′ NCR of poliovirus RNA. This structure has been confirmed, in part, by RNase and chemical-probing experiments. The numbering refers to the poliovirus type 1 RNA genome. The seven stem-loop structures have been labeled A through G. The asterisks indicate AUGs conserved among the entero- and rhinoviruses. The linker scanning mutations of this study are located exclusively in stem-loops F and G, which contain the putative internal ribosome-binding site. The conserved polypyrimidine tract is located at nt 588 and is separated by 22 nt from the cryptic $AUG_{586}$. The figure is modified from a structure suggested by Jackson and colleagues (13).

subunits has been called the "ribosome landing pad" (41). The analogous region of the EMCV 5′ NCR is referred to as the internal ribosome entry site (IRES) (13, 14), a term employed in the present communication.

Recently, several cellular proteins which interact with the 5′ NCR of picornavirus RNAs and may play a role in translation initiation were identified. A 50-kDa protein of cellular origin was shown to bind to a stem-loop present at nt 186 to 221 in the 5′ NCR of poliovirus RNA (6, 35). A factor present in HeLa cells, p52, was shown by UV cross-linking to bind to a computer-predicted stem-loop at nt 559 to 624 in the poliovirus 5′ NCR (32). By employing a UV cross-linking assay, a cellular 57-kDa protein present in rabbit reticulocyte lysate was shown to interact with a segment of EMCV RNA that contains the IRES (17). Homology to known translation initiation factors has not been reported for the p50, p52, and p57 cellular factors.

It is assumed that proteins bind to RNA as a result of their recognition of either specific nucleic acid sequences or secondary-structure motifs. Deletion and point mutation analyses of the picornavirus 5′ NCR polypyrimidine tract in vitro and in vivo suggest that this sequence represents an important signal for translation initiation, although it appears not to be directly involved in factor binding (31, 36, 42). A recent model proposed by Jang and colleagues, however, stresses the importance of the distance between the polypyrimidine tract present at nt 558 and an AUG at nt 586 in the 5′ NCR of poliovirus RNA (16). Indeed, if the distance of 22 nt is altered, translational efficiency decreases (44). This suggests that factors may exist which are capable not only of recognizing specific sequences and secondary structures but which also require the proper spacing of these entities.

In this study, we employed an approach that was originally used to define the essential features of a eukaryotic RNA polymerase II promoter (30) to document the importance of the RNA secondary structure of the 5′ NCR and the RNA-RNA and RNA-protein interactions occurring in the poliovirus IRES which mediate internal ribosome entry. We generated 14 linker scanning mutations in the IRES of poliovirus RNA between nt 472 and 615 that neither deleted nor added any nucleotides. Instead, these mutations substituted precisely 8 nt of the viral sequence with those of a synthetic linker. The linker scanning mutations produced the following three classes of phenotypes: infectious constructs resulting in temperature-sensitive or wild-type-like viruses and noninfectious constructs. We analyzed the phenotypes of the mutant viruses and attempted to define the defects of the noninfectious constructs. By employing electrophoretic mobility shift assays, we focused on the RNA-protein interactions occurring in the most distal stem-loop of the 5′ NCR. We show that factor binding may be a function of the distance between the polypyrimidine tract present at nt 558 and the AUGs at nt 586 and 743.

## MATERIALS AND METHODS

**Construction of the linker scanning mutations as subgenomic and full-length cDNAs.** The method used for constructing the linker scanning mutations was as described previously (30), with slight modifications (9). To construct the 3′ deletions, a pGEM1-based plasmid (pT7-5′NCR) containing the 5′ NCR of PV1 (nt 1 to 745) was linearized at the *Bsm*I site (nt 456). The linearized DNA was digested with *Bal* 31 (0.8, 0.4, or 0.2 U per 10 μg of DNA) at 30°C for 10 min to generate various size deletions. Following phenol-chloroform extraction, the DNA was treated with the Klenow fragment of DNA polymerase to create uniformly blunt ends to which synthetic *Xho*I linkers were ligated with T4 DNA ligase. The extent of the deletions was defined by dideoxynucleotide sequencing of alkali-denatured plasmid DNA with Sequenase (U.S. Biochemicals). The 5′ deletions were produced in the same manner, except that the DNA was linearized at *Bal*I (nt 627). Another smaller set of 3′ and 5′ deletions was made by linearizing at *Nco*I (nt 388) and *Pfl*MI (nt 497). Matching sets of 5′ and 3′ deletions that were separated only by the 8-bp *Xho*I linker were joined at the *Xho*I site to generate complete linker scanning mutations. These were then reconstructed into pT7-PV1, a full-length cDNA plasmid of PV1. The plasmid pT7-PV1 was constructed by ligating a 2.7-kb *Bsm*I-*Eco*RI vector fragment derived from pT7-PV1.8 which also contains PV1 sequences from nt 1 to 456, a 1.1-kb *Bsm*I-*Bsm*I fragment of PV1 sequences from nt 456 to 1513, and a 6-kb *Bsm*I-*Eco*RI fragment of PV1 sequences. The 1.1- and the 6-kb fragments were derived from pPVA55 (24). The full-length cDNAs containing the linker scanning mutations were constructed by ligating a ~200-bp *Bsm*I (nt 456)-*Bam*HI (nt 670) fragment derived from the subclone containing the linker scanning mutation, an 800-bp *Bam*HI (nt 670)-*Bsm*I (nt 1513) fragment derived from pT7-PV1, and an 8.8-kb *Bsm*I (nt 1513)-*Bsm*I (nt 456) fragment containing PV1 sequences in addition to the vector sequences. The locations of the linker scanning mutations were confirmed by DNA sequence analysis.

**Construction of the stem-loop G vector.** A vector into which different DNA fragments can be cloned for generation of transcripts to be subsequently used in electrophoretic mobility shift assays was generated. A 2.2-kb *Bsm*I (nt 456)-*Aat*II (nt 2089 in pGEM1, blunt ended with Klenow

enzyme) fragment derived from pT7-5NC-X564 containing the *Xho*I linker scanning mutation at nt 563, two synthetic oligonucleotides reconstructing the T7 promoter, and two synthetic oligonucleotides creating a new *Sac*I site at the very 5′ end of the transcriptional start site were ligated to produce the transcription vector pT7-GSF. This vector was digested with the restriction endonucleases *Xho*I and *Sac*I and treated with the Klenow enzyme. A 2.1-kb fragment of this linear DNA was gel purified and incubated with T4 DNA ligase, creating the transcription vector pT7-GSG, which, when linearized at the *Bal*I (nt 627) restriction endonuclease site, directs the synthesis of stem-loop G RNA (nt 572 to 627).

**In vitro transcription of subgenomic and full-length poliovirus cDNA.** The subgenomic cDNAs were linearized by digestion with restriction endonuclease *Sna*BI (nt 2954) within the P1 coding region. In vitro transcriptions were carried out with bacteriophage T7 RNA polymerase (Pharmacia) as described elsewhere (27), except that RNAs were treated with RNase-free DNase, and ethanol precipitated a second time to ensure removal of the DNA template and all free nucleotides. Restriction endonuclease *Eco*RI was used to linearize full-length poliovirus cDNAs. The linearized full-length poliovirus cDNAs were transcribed with bacteriophage T7 RNA polymerase (48), and the synthesized RNAs were used to transfect HeLa cell monolayers without purification.

**In vitro translation of mutant RNAs.** RNAs containing the linker scanning mutations were translated in the presence of [$^{35}$S]methionine at 30°C in a rabbit reticulocyte lysate (Promega) supplemented with ~15 to 20% (vol/vol) of a HeLa cell cytoplasmic extract (48). The RNA concentration in the translation reaction mixtures was 6 μg/ml. Translation reactions were terminated after 2 h by incubation at 30°C with RNase A (200 μg/ml) for 20 min. All reaction mixtures were diluted 10-fold in Laemmli sample buffer and analyzed by sodium dodecyl sulfate (SDS)-polyacrylamide gel electrophoresis (25). Autoradiograms of the gels were scanned with an LKB Ultrascan 2 laser densitometer.

**Transfection of RNAs derived from full-length poliovirus cDNAs.** HeLa cell monolayers on 60-mm-diameter plates that were 80% confluent were transfected with in vitro-transcribed RNA (1 to 5 μg) from full-length cDNAs by a modified DEAE–dextran-mediated transfection technique (26, 47). HeLa cell monolayers were rinsed with 2 ml of TS buffer (137 mM NaCl, 4.4 mM KCl, 0.7 mM $Na_2HPO_4$, 25 mM Trizma base, 5 mM $MgCl_2$, 0.3 μM $CaCl_2$), treated with 0.25 ml of 1 mg of DEAE-dextran per ml and RNA in TS buffer, incubated at room temperature for 30 min, and overlaid with either Dulbecco modified Eagle medium containing 10% fetal calf serum or a semisolid medium consisting of Dulbecco modified Eagle medium, 6% fetal calf serum, and 0.45% agarose. The transfected monolayers were incubated at 33 and 37°C until cytopathic effects or plaques were visible.

**Virus stock preparation and plaque assay.** Mutant virus stocks were prepared either by picking well-isolated plaques 2 to 3 days after transfection or by harvesting liquid overlays 2 to 3 days after transfection. Liquid overlay harvests were used to infect fresh HeLa cell monolayers, which were then overlaid with semisolid medium. Well-isolated plaques were then picked as described above. The plaques were clonally purified by a second round of infection and plaque isolation. The plaque-purified stock was expanded by two serial passages through HeLa cell monolayers. The titers of the stocks were determined on 60-mm-diameter plates of HeLa cell monolayers under semisolid medium at 33 or 37°C.

**One-step growth curves.** The kinetics of mutant viral growth and wild-type viral growth were measured as described previously (3), with some modifications. Briefly, suspension cultures of HeLa cells were infected with poliovirus type 1 or mutant polioviruses at a multiplicity of infection of 15 for 30 min at room temperature. Then, the cells were rinsed three times with isotonic phosphate-buffered saline and the infected cultures were incubated at 33 and 39°C. Supernatant and cells were harvested together at 2, 3, 4, 5, and 6 h at 39°C and at 2, 4, 6, 8, and 10 h at 33°C. The number of PFU per cell present at each time point was determined by plaque assay.

**Sequencing of viral RNAs.** Viral RNA was prepared by the Nonidet P-40 lysis method (5). The viral RNA was sequenced by extension of a synthetic primer corresponding to nt 630 to 650 or to nt 412 to 430 of poliovirus RNA with [α-$^{32}$P]dATP, a mixture of deoxynucleotides and dideoxynucleotides, and reverse transcriptase (10, 45).

**PCR to reconstruct the isolated viral revertants.** The viral RNA was isolated as described above. The polymerase chain reaction (PCR) method was carried out as described before (19), with the following modifications. To generate the first cDNA strand, deoxynucleotides (2 mM), RNasin (50 U), 50 μg of RNA, and 15 pmol of the synthetic primer were assembled in 1× reverse transcriptase buffer (50 mM Tris-HCl [pH 8.3], 10 mM $MgCl_2$, 0.4 mM dithiothreitol, 80 mM KCl), to which avian myeloblastosis virus reverse transcriptase (100 U) was added. The reaction mixture was incubated for 2 h at 42°C, phenol-chloroform extracted, and ethanol precipitated. The newly generated cDNA was then mixed in 1× PCR buffer (50 mM KCl, 10 mM Tris-HCl [pH 8.4], 2.5 mM $MgCl_2$), with two synthetic primers (one annealing to nt 412 to 430 and the other annealing to nt 1812 to 1832 at the opposite end of the PV1 cDNA), 2 μg of gelatin per μl, 2 mM deoxynucleoside triphosphates, and 2 U of *Taq* polymerase. The mixture was overlaid with mineral oil and incubated for 25 cycles in a COY Tempcycler. After the PCR reaction was complete, the DNA was phenol-chloroform extracted, ethanol precipitated, and analyzed on an agarose gel. A 260-bp fragment was gel purified after digestion with *Bsm*I (nt 456) and *Taq*I (nt 866). This fragment, together with an ~8.5-kb *Bsm*I (nt 1513)-*Bsm*I (nt 456) vector fragment and a 647-bp *Taq*I (nt 866)-*Bsm*I (nt 1513) fragment, both derived from pT7-PV1, was used to reconstruct the mutations in full-length poliovirus cDNA.

**HeLa cell cytoplasmic extract preparations.** Preparation of HeLa S10 extract has been previously described (4). Ribosomal salt wash and ammonium sulfate fractionations were prepared essentially as described before (11), except that the final dialysis was in a mixture containing 100 mM potassium acetate, 20 mM HEPES (*N*-2-hydroxyethylpiperazine-*N*′-2-ethanesulfonic acid; pH 7.5), 1 mM dithiothreitol, and 0.2 mM EDTA.

**Electrophoretic mobility shift assays.** Assays were performed as described previously (20) with some modifications. The radioactively labeled RNAs used in this binding assay were generated by in vitro transcription of the vector pT7-GSG (as described above), which was linearized with the restriction endonuclease *Bal*I (nt 627). tRNA (10 μg) was incubated with 10 or 20 μg of HeLa B cut in binding buffer (25 mM KCl, 5 mM HEPES, 2 mM $MgCl_2$, 0.1 mM EDTA, 3.8% glycerol, 2 mM dithiothreitol), pH 7.5, for 10 min at 30°C. Then, 0.5 pmol of the labeled RNA (nt 572 to 627) was added, and the solution was incubated for 10 min at 30°C.

Next, 2.5 μg of heparin was added to the binding reaction mixture for 10 min at 30°C. Finally, glycerol was added to 10%, and the free and bound RNAs were separated on a native 0.5× Tris-borate-EDTA–6% polyacrylamide (40:1) gel containing 5% glycerol. The competitor RNAs were generated by in vitro transcription of the subgenomic cDNAs containing the mutant 5′ NCRs (nt 1 to 747) of poliovirus RNA. They were added at a 5- or 40-fold molar excess to the first incubation period.

## RESULTS

**Characterization of the linker scanning mutants.** In previous studies, the 5′ NCR of poliovirus RNA has been genetically altered by deleting or inserting nucleotides which, in turn, altered the nucleotide spacing and/or the secondary structure of the 5′ NCR (Fig. 1). Since the biological activity encoded in the 5′ NCR may depend on proper spacing, we employed an approach which would conserve the spacing of the secondary structure of the 5′ NCR. We generated 14 linker scanning mutations in the 5′ NCR (as described in Materials and Methods) in the region containing the putative IRES by precise substitution of viral sequences with a synthetic *Xho*I linker. The linker scanning mutations are located between nt 472 and 615, a region of the viral RNA that encompasses stem-loops F and G (Fig. 1). Such linker substitutions would be expected to have an effect on viral functions if the altered sequence disturbs the stability of a stem or the recognition of a single-stranded RNA region involved in factor binding or RNA-RNA interactions. To better predict the effects of these mutations on the viral functions, we examined the sequence substitutions within the context of their computer-predicted secondary structures. A total of 11 of the linker scanning mutations alter sequences in stem-loop F, and with the exception of X515, all of them would be predicted to perturb base-paired regions (Fig. 2A and B). Thus, if stem stability is important for viral functions, it might be expected that most of these mutations would severely impair viral processes like translation initiation or RNA synthesis. Three linker scanning mutations are located in stem-loop G (Fig. 2C). The lesion X564 substitutes sequences in the conserved polypyrimidine tract, while mutations X585 and X607 would be predicted to perturb the most distal hairpin structure (stem-loop G [Fig. 1]).

The mutant viral mRNAs, generated by in vitro transcription, were transfected into HeLa cells and assayed for virus production at two temperatures (33 and 37°C). The locations of the linker scanning mutations in the viral RNAs were confirmed by RNA sequence analysis. The mutations X472, X478, and X482 are located in a region thought to contain determinants for the attenuation and/or neurovirulence phenotype of poliovirus (8, 33). All three mutations perturb the base pairing of a short internal stem, and all three are lethal (Fig. 2A). The sequence substitution of the linker scanning mutation X515 occurs in a predicted single-stranded loop (Fig. 2A). This loop may constitute a protein binding site or be involved in RNA-RNA interactions stabilizing a higher order structure. The resulting temperature-sensitive virus is impaired for growth at the nonpermissive temperature (39°C), as demonstrated by a reduction of 3 log units in virus yield compared with that of the wild-type virus (Fig. 3A). The mutations X520, X521, and X522 would be predicted to severely affect stem stability, and, indeed, they are not infectious. The importance of the stability of this stem is further emphasized by mutation X527, which produced a temperature-sensitive virus isolate. The affected stem normally contains 6 bp but can form only 4 bp with the *Xho*I linker substitution. The loss of two G-C base pairs can considerably destabilize a stem and may introduce a conformational change in the 5′ NCR that impairs viral functions. A one-step growth analysis of X527 demonstrated a 4-log-unit reduction in virus yield at 39°C compared with that of the wild type. At 33°C, only a 1-log-unit reduction in X527 virus growth was observed (Fig. 3B).

Additional evidence for base-paired structures in stem-loop F is provided by mutations X529 and X539. Both lesions should disrupt some internal base pairing and additionally change sequences in predicted single-stranded regions. The destabilization of the secondary structure caused by both mutations, perhaps coupled with alterations in sequences of single-stranded regions, makes them noninfectious constructs. Transfection of HeLa cells with RNAs containing the linker scanning mutation X543, which is also located in stem-loop F, results in the production of a mutant virus severely impaired for growth at 33°C. We were unable to isolate a virus containing this lesion at a higher temperature (39°C). Not surprisingly, a one-step growth analysis revealed a dramatic decrease (3.5 log units) in virus yield compared with that of the wild-type virus at 33°C, the permissive temperature (Fig. 3C). This mutant virus, Se1-5NC-X543, is severely impaired in translation initiation and, perhaps, other viral functions (see below). The introduced linker sequences of X543 destabilize a short stem structure (Fig. 2B), which has a dramatic effect on viral functions. A fortuitously isolated point mutation, N549, which disrupts the same stem as X543, appeared to produce a virus with a wild-type growth phenotype (see below).

The final three linker scanning mutations are predicted to alter sequences in stem-loop G, as shown in Fig. 2C. Sequences in the polypyrimidine tract were substituted by the mutation X564. A virus with a wild-type phenotype was isolated following transfection of synthetic RNAs containing the X564 lesion. Apparently, sequences at the 3′ end of the C- and U-rich motif can be altered without a detectable loss of virus viability. The construct X585 altered sequences in the conserved octamer within stem-loop G and changed the conserved upstream AUG at 586 to CUC. A total of 4 bp could not be formed in the predicted hairpin structure of RNAs containing the X585 mutation. We were unable to isolate a virus containing the original X585 lesion at either 33 or 37°C. Finally, the linker scanning mutation X607 is located on the opposite side of the predicted hairpin in stem-loop G. Although this mutation should also perturb base pairing within the secondary structure, a virus with a wild-type growth phenotype was isolated following RNA transfection. This result suggests that for stem-loop G, the secondary structure may not be as important as the precise nucleotide sequences.

**In vitro translation properties of mRNAs derived from cDNAs containing the linker scanning mutations.** To determine whether the introduced mutations would cause specific defects in translation initiation of poliovirus RNA, RNAs truncated in the coding region for the polyprotein and containing the individual linker scanning mutations were assayed in vitro in a rabbit reticulocyte lysate cell-free translation system as described in Materials and Methods. The translation products were resolved on an SDS–10% polyacrylamide gel (Fig. 4). The autoradiograph was analyzed by laser densitometric scanning to precisely quantitate translation efficiencies of the mutant RNAs (Table 1). A similar translation pattern was observed when the mutant

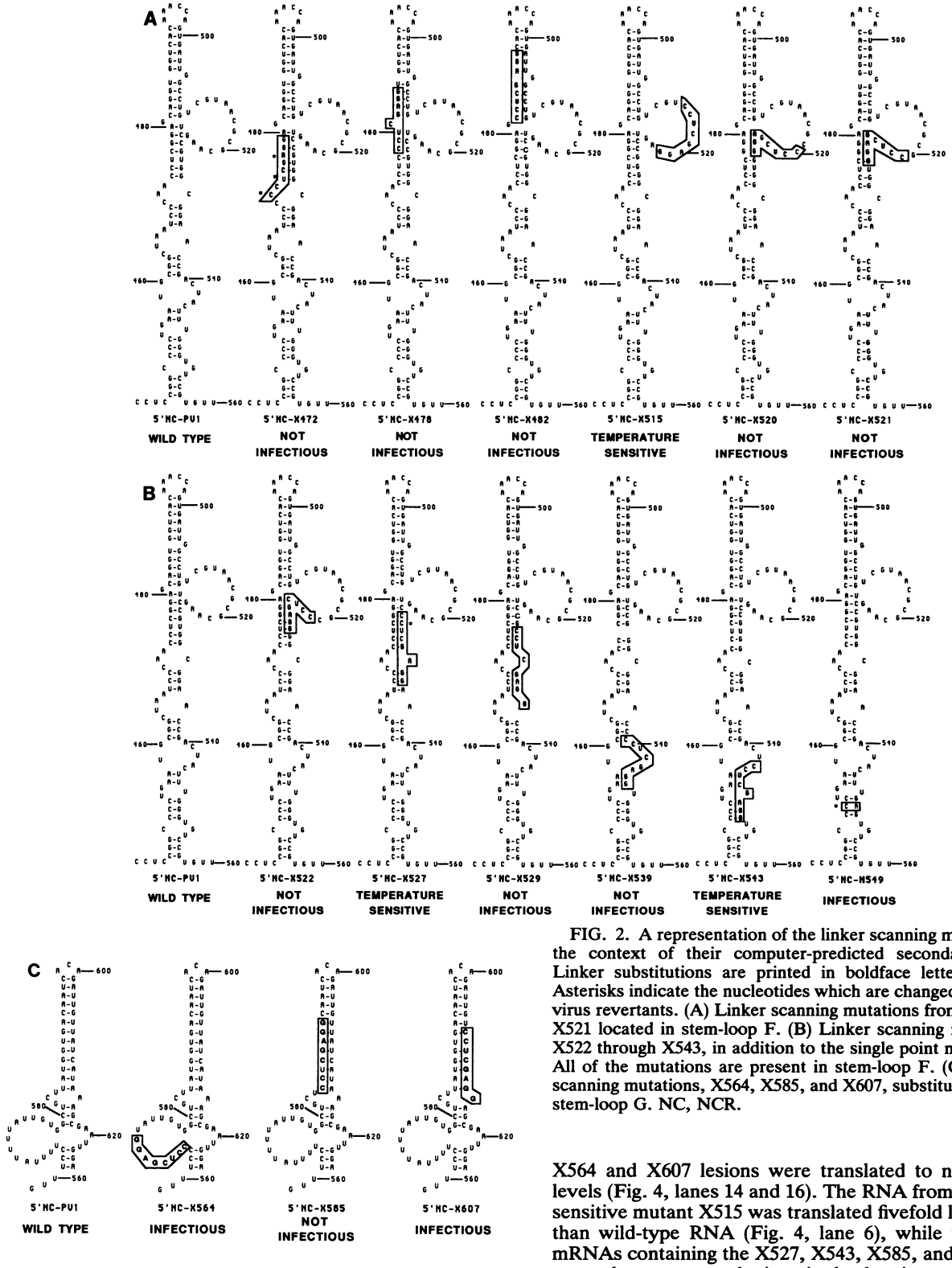


FIG. 2. A representation of the linker scanning mutations within the context of their computer-predicted secondary structures. Linker substitutions are printed in boldface letters and boxed. Asterisks indicate the nucleotides which are changed in the isolated virus revertants. (A) Linker scanning mutations from X472 through X521 located in stem-loop F. (B) Linker scanning mutations from X522 through X543, in addition to the single point mutation, N549. All of the mutations are present in stem-loop F. (C) Three linker scanning mutations, X564, X585, and X607, substitute sequences in stem-loop G. NC, NCR.

RNA transcripts were translated only in HeLa S10 extract (data not shown). The efficiency of in vitro translation initiation for most of the linker scanning mutations correlated well with the results obtained following RNA transfection of cultured HeLa cells. Thus, mRNAs containing the X564 and X607 lesions were translated to near wild-type levels (Fig. 4, lanes 14 and 16). The RNA from temperature-sensitive mutant X515 was translated fivefold less efficiently than wild-type RNA (Fig. 4, lane 6), while translation of mRNAs containing the X527, X543, X585, and N549 lesions seemed more severely impaired, showing a >10-fold decrease in protein synthesis levels (Fig. 4, lanes 10, 13, 15, and 17, respectively). Transcripts corresponding to all of the lethal mutations, X472, X478, X482, X520, X521, X522, X529, and X539 (Fig. 4, lanes 3, 4, 5, 7, 8, 9, 11, and 12, respectively), directed low levels of protein synthesis, barely

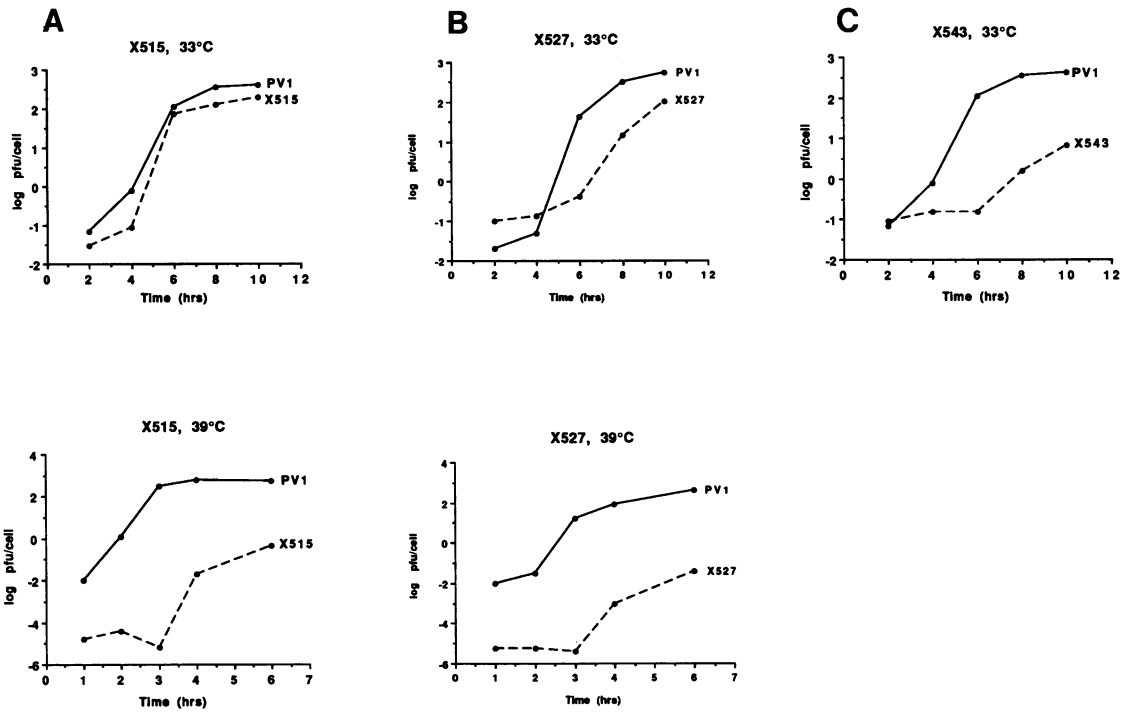


FIG. 3. Kinetics of virus production in HeLa cells infected with Sel-5NC-X515 (A), Sel-5NC-X527 (B), or Sel-5NC-X543 (C) or with wild-type poliovirus at 33 and 39°C. Suspension cultures of HeLa cells with a cell density of $6 \times 10^5$ cells per ml were infected at a multiplicity of infection of 15 with the mutant or the wild-type virus and incubated for 30 min at room temperature. The cells were harvested every 2 h for the infection at 33°C and every hour for the infection at 39°C. The numbers of PFU per cell were determined by plaque assays as described in Materials and Methods. Solid lines, wild-type poliovirus; dashed lines, mutant viruses. Note that no virus was recovered for mutation 5NC-X543 at 39°C.

above the level of the Δ450 construct, which has the entire stem-loop F (from nt 445 to 558) deleted (Fig. 4, lane 18). Full-length synthetic mRNAs containing the Δ450 deletion were unable to produce infectious virus following transfection of HeLa cells. In the context of the in vitro translation assay, shown in Fig. 4, the RNA containing the Δ450 deletion can be considered a translation-negative control.

TABLE 1. Relative translational efficiencies of the mutant constructs truncated in the P1 region of the poliovirus genome and the infectious virus production of the same mutations in full-length viral RNAs

| RNA template | Relative translational efficiency[a] | Infectious virus[b] |
|---|---|---|
| Wild type | +++++ | Yes (wt) |
| X564 and X607 | +++ | Yes (wt), yes (wt) |
| X515 | ++ | Yes (ts) |
| X527, X543, N549 | + | Yes (ts), yes (ts), yes[c] |
| X585 | + | No |
| X472, X478, X482 | − | No, no, no, no, no, no |
| X520, X521, X522 | − | No, no, no |
| X529, X539, and Δ450 | − | No, no, no |

[a] This column summarizes the trends observed from two separate translation experiments of each RNA. The autoradiographs were quantitated by laser densitometric scanning. +++++, wild-type levels, set at 100%; +++, 50 to 80% of wild-type levels; ++, 20 to 40% of wild-type levels; +, ~10% of wild-type levels; −, <5% of wild-type levels.

[b] wt, wild type; ts, temperature sensitive.

[c] The 37°C virus stock of Sel-5NC-N549 (which is not temperature sensitive) already contains the compensatory base change at nt 453.

The in vitro protein synthesis levels directed by the RNAs containing the X543 and N549 lesions did not correlate precisely with their in vivo phenotypes (Fig. 4, lanes 13 and 17). The point mutation N549 exhibited a wild-type-like growth phenotype, but its RNA was translated at low levels. The viral RNA of mutant Sel-5NC-N549 (containing the N549 mutation) may have a second site reversion(s) in its genome which allowed it to be translated efficiently in vivo (see below). Synthetic RNAs containing the X543 mutation were translated at levels which are similar to those observed for RNAs that yield mutant virus upon transfection at 37°C. However, virus was recovered only at 33°C. The in vitro translation assay employed in this study cannot be used to identify temperature-sensitive translation functions, since in vitro translations at elevated temperatures (37 or 39°C) are inefficient, even with wild-type poliovirus RNAs (unpublished observations). When we analyzed the kinetics of RNA synthesis of the mutant virus Sel-5NC-X543 at 33, 37, and 39°C, RNA synthesis was severely impaired at 37 and 39°C, while it was only delayed at 33°C (data not shown). These data are consistent with the data from RNA transfections with X543-containing transcripts, in which virus could be recovered only at 33°C. Thus, it appears that the X543 lesion affects both the translation and the RNA replication properties of the viral RNA, possibly as a result of a global defect in RNA-protein interactions.

**Isolation of revertants to determine structure-function relationships of the poliovirus 5′ NCR.** In order to further define the sequence and/or structure determinants in stem-loops F and G within the poliovirus 5′ NCR, we carried out nucleotide sequence analysis of pseudorevertants generated from

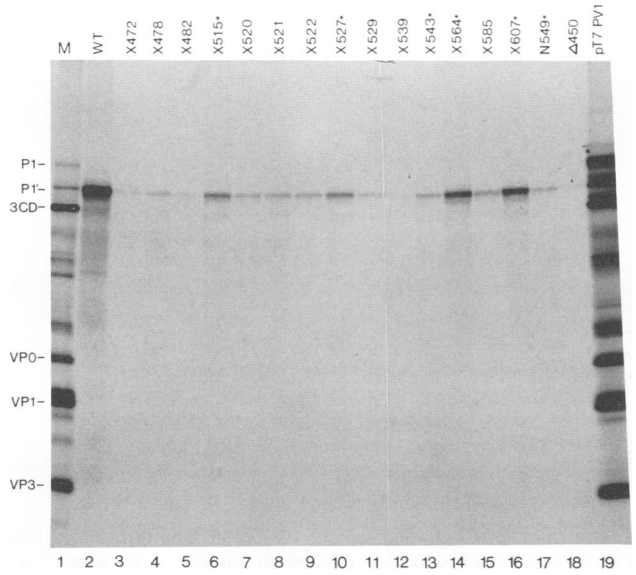


FIG. 4. In vitro translation of mutant and wild-type transcripts in a rabbit reticulocyte lysate supplemented with a HeLa S10 extract. The cDNA templates were truncated within the P1 region. Transcripts derived from these templates were translated in vitro as described in Materials and Methods. The translation products were resolved on an SDS–10% polyacrylamide gel. M, marker lane of [$^{35}$S]methionine-labeled poliovirus proteins from HeLa cell monolayers infected with wild-type poliovirus. Asterisks indicate constructs from which viruses were isolated. Designations above the lanes refer to the different wild-type (WT) or mutant constructs. The plasmid pT7-PV1 is a full-length cDNA of the wild-type poliovirus type 1, and Δ450 is a construct that has stem-loop F deleted.

some nonviable constructs and mutant viruses containing the *Xho*I linker replacements. The second-site mutations found in isolated viral revertants revealed a specific sequence requirement of the RNA genome which is necessary for either secondary-structure formation or factor binding. Transfection of RNAs encoding several of these linker scanning mutations did not result in virus isolates containing the original lesion but instead incorporated reversion mutations. A revertant was isolated for X472 at each transfection temperature. At 33°C, a single nucleotide ($U_{474}$→C) within the introduced *Xho*I linker was substituted, such that an additional base pair could be formed. This implies that stem stability is important to virus viability (Fig. 2A). Two single nucleotide changes were observed in X472 at 37°C ($C_{472}$→U and $A_{477}$→C). Both substitutions altered nucleotides within the linker sequence, but only the change at position nt 477 allows additional base pair formation. nt 472 in poliovirus type 1 is in an unpaired loop region in the predicted wild-type structure. nt 474 and 477 are both present in base-paired stems (note that in poliovirus type 3, nt 472 is base paired). A revertant was also isolated at 37°C from the temperature-sensitive virus Sel-5NC-X527 which contained a single nucleotide change in the introduced linker ($C_{528}$→G) to enable base pairing of the predicted stem structure (see asterisk in secondary structure of X527 in Fig. 2B), suggesting that the temperature-sensitive phenotype is at least partly due to the instability of secondary structures. In addition, sequence analysis of the RNA of the mutant virus Sel-5NC-N549 (containing a single point mutation at nt 549), grown at 37°C, identified a compensatory nucleotide change at position $C_{453}$→U that permitted the formation of a base pair with the original mutation at nt 549 which stabilizes a short stem structure. Such a second-site mutation could account for the recovery of a virus with nearly wild-type properties, even though the primary transcript containing the original single-nucleotide change was translated at levels that were ~10% of wild-type levels. Thus, the sequence analysis of revertants provided additional confirmation of the structural requirements of the 5′ NCR necessary for efficient translation initiation. These single-point-reversion mutations imply that the stability of secondary structures in stem-loop F, rather than the nucleotide sequence, is of primary importance for either ribosome binding or the interaction with facilitating factors.

Of particular interest were the results we obtained following sequence analysis of the revertant viruses recovered after transfection of synthetic RNAs containing the lethal lesion X585. Surprisingly, revertants of X585 isolated at 33 and 37°C revealed a gross deletion in the poliovirus 5′ NCR of ~150 nt, eliminating the entire stem-loop G. The virus recovered at 37°C contained a deletion that spans from nt 563 to 716 (X585$\Delta_1$) (Fig. 5), while the virus recovered at 33°C had deleted sequences from nt 570 to 729 (X585$\Delta_2$). The 5′ half of the conserved polypyrimidine tract is preserved in both of the isolated revertants of X585, but the AUG at nt 586 is eliminated. A [$^3$H]uridine incorporation experiments which measures the levels of viral RNA synthesis, in cells infected with the revertant virus Sel-5NC-X585$\Delta_1$ showed viral RNA levels (and kinetics) similar to those of wild type at 33, 37, and 39°C. The only notable difference in this analysis was that RNA synthesis at 33°C was slightly delayed for Sel-5NC-X585$\Delta_1$ (data not shown). To ascertain that the wild-type phenotype of Sel-5NC-X585$\Delta_1$ was not due to second-site lesions at other locations in the viral RNA genome, the gross deletion of X585$\Delta_1$ was reconstructed by cDNA synthesis and PCR amplification and reintroduced into a full-length cDNA copy of PV1. This reconstructed revertant, X585R, was transcribed in vitro, and the mutant RNA was transfected into HeLa cells. Again, a virus with a wild-type phenotype was produced, as determined by measuring the kinetics of RNA synthesis (data not shown). The isolated revertant Sel-5NC-X585$\Delta_1$ and the reconstructed revertant Sel-5NC-X585R display identical profiles of RNA synthesis which resemble those of wild-type poliovirus. As previously shown in Fig. 4, RNA derived from the linker scanning mutation X585 was not translated efficiently in vitro (Fig. 6, lane 3). However, the reconstructed revertant X585R containing the stem-loop G deletion is translated to wild-type levels (Fig. 6, lane 4). These results suggest that the presence of stem-loop G is not essential for translation initiation and raise the possibility of functional redundancy or sequence and/or spacing flexibility within the region between nt 560 and 743 of the poliovirus genome.

**RNA-protein interactions involving stem-loop G.** RNA-protein interactions involving a cellular protein (called p52) were previously shown by UV cross-linking to occur within stem-loop G sequences (32). It was of interest to analyze such RNA-protein interactions with stem-loop G in the context of the linker scanning mutations which affect this part of the poliovirus 5′ NCR. We performed electrophoretic mobility shift assays using an in vitro-transcribed RNA containing poliovirus sequence from nt 572 to 627 (Fig. 7). The factor p52 had been previously shown to be abundant in a crude HeLa cytoplasmic extract (32). In our binding studies, we used a fractionated extract, B cut (40 to 70% ammonium sulfate fractionation), of a HeLa ribosomal salt

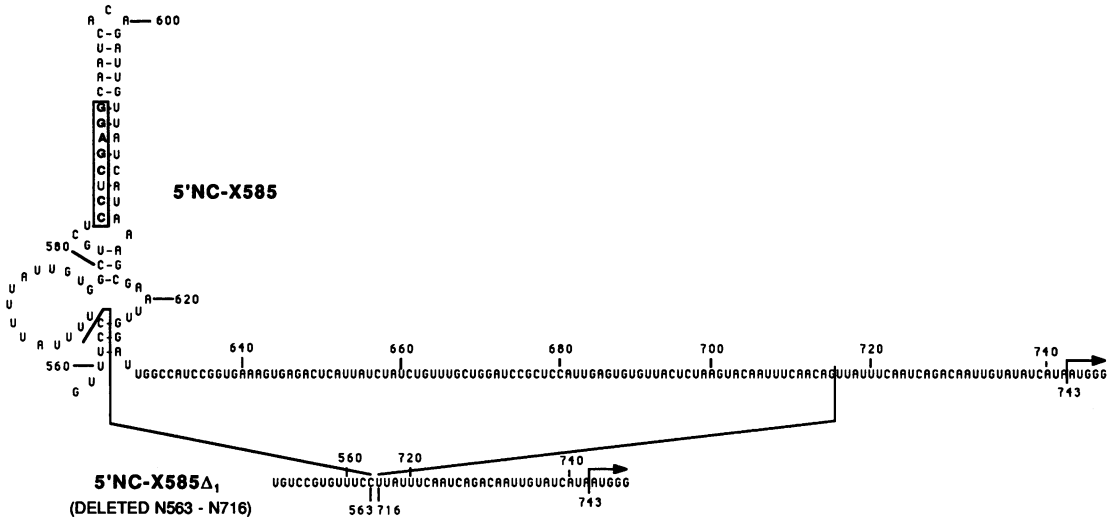


FIG. 5. A diagram of the predicted secondary structure of stem-loop G of the linker scanning mutant PV1X585. The introduced linker sequence is printed in boldface letters and boxed. A virus containing this exact lesion was never isolated. Instead, a revertant virus, Sel-5NC-X585$\Delta_1$, which contained a gross deletion in its RNA genome from nt 563 to 716, was recovered at 37°C. The authentic translation start site is at nt 743.

wash which is enriched for a number of translation initiation factors (11). No detectable binding activity was observed with an A cut (0 to 40% ammonium sulfate fractionation) of a HeLa ribosomal salt wash (data not shown). The free and bound RNAs were resolved on a 6% polyacrylamide nondenaturing gel. The free RNA (Fig. 7, lane 1) migrates faster than the RNA-protein complex formed upon addition of increasing amounts of HeLa B cut (lanes 2 and 3). Synthetic RNAs containing the linker scanning mutations were used as competitor RNAs to further define the binding sites of the factor(s) which interacts with stem-loop G. As expected, the wild-type 5′ NCR RNA competes for the entire complex at a 40-fold molar excess (Fig. 7, lanes 4 and 5). The 5′ NCR of X564, derived from a mutant virus displaying a wild-type phenotype, competes for the bound protein(s) as efficiently as wild type (Fig. 7, lanes 6 and 7). The linker scanning lesion X585 5′ NCR RNA is not capable of reducing the levels of RNA-protein complex formation, even at a 40-fold molar excess (Fig. 7, lanes 8 and 9). This result is not surprising, since RNA containing the X585 lesion is not infectious and does not efficiently direct translation initiation in vitro. The 5′ NCR of X607, which contains the linker substitution in the hairpin structure located on the opposite side of the X585 lesion, does not compete for factor binding (Fig. 7, lanes 10 and 11), although a virus with a wild-type phenotype containing the X607 mutation was isolated. The reconstructed revertant, X585R, which has the G stem-loop deleted, was also tested as a competitor. Surprisingly, this construct competed efficiently for the bound protein(s) at a 40-fold molar excess (Fig. 7, lanes 12 and 13). To further confirm the specificity of the observed RNA-protein interactions, we used an RNA (nt 543 to 750) containing the lesion of X585R1 in electrophoretic mobility shift assays. This RNA is capable of specific complex formation with HeLa B-cut extracts (data not shown). These results suggest that disruption of base pairing in the stem structure in stem-loop G eliminates RNA-protein interactions from this segment of the 5′ NCR. However, complete deletion of the stem-loop G sequences, as well as adjacent sequences not predicted to form a stable secondary structure, does not interfere with the formation of an RNA-protein complex that appears to be functionally analogous to that directed by stem-loop G.

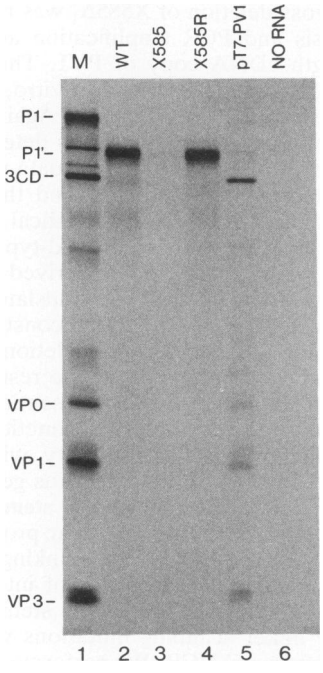


FIG. 6. In vitro translation of the P1 truncated RNAs containing the lesions X585 and X585R. The in vitro transcription and in vitro translation conditions are described in Materials and Methods. Samples were diluted in Laemmli buffer and resolved on an SDS–10% polyacrylamide gel. Lanes: M, wild-type poliovirus-infected HeLa cell marker; 5, a full-length poliovirus RNA translation; NO RNA, no RNA was added to the in vitro translation reaction.

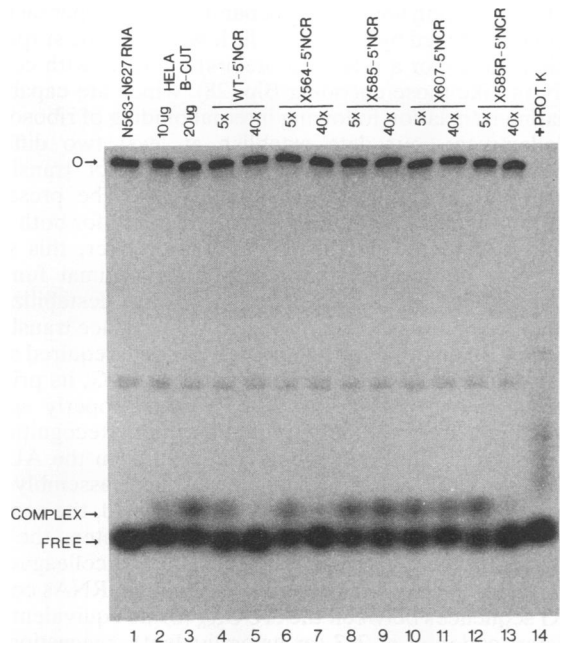


FIG. 7. Interaction of a cellular protein(s) with sequences from nt 572 to 627 in poliovirus RNA. The electrophoretic mobility shift with stem-loop G RNA and HeLa cell extract (B cut of ribosomal salt wash fraction) was carried out as described in Materials and Methods. The RNA was generated in vitro as described in Materials and Methods. This RNA (N563-N627 RNA) contains *Xho*I linker sequences up to nt 571 and poliovirus sequences from nt 572 to 627. Radiolabeled RNA molecules were incubated in the absence or in the presence of HeLa cell extract. A 5- or 40-fold molar excess of unlabeled competitor RNA molecules was added, and the migration of unbound (free) RNA and specific RNA-protein complexes was analyzed on a native 0.5× Tris-borate-EDTA–6% polyacrylamide (40:1) gel. Reaction mixtures contained the following competitor RNA molecules: no competitor RNA (lane 1), nonspecific competitor tRNA (lanes 2 and 3), wild-type virus 5′ NCR RNA (lanes 4 and 5), X564 5′ NCR RNA (lanes 6 and 7), X585 5′ NCR RNA (lanes 8 and 9), X607 5′ NCR RNA (lanes 10, 11), and X585R1 5′ NCR RNA (lanes 12 and 13). The reaction mixture shown in lane 14 included proteinase K to show that the complex formed was due to an RNA-protein interaction.

## DISCUSSION

In this study, we have analyzed the structure and/or function relationships of the internal ribosome entry site of the 5′ NCR of poliovirus RNA. We generated 14 linker scanning mutations in stem-loops F and G of the 5′ NCR of poliovirus RNA which contained neither deletions nor insertions. Thus, any observed defects of functions required for a successful viral life cycle will be due to a structural disturbance of base-paired stems or to the abolishment of factor binding because of an altered nucleotide sequence. Our results suggest that stem-loop F is very sensitive to nucleotide changes which destabilize secondary structures. Most of the linker scanning mutations in this stem-loop decrease the number of paired bases (e.g., X472, X478, X482, X520, X521, X522, X527, X529, X539, and X543) within a stem, thereby decreasing the stability of the proposed secondary structure. Only three of the linker scanning mutations within stem-loop F, X515, X527, and X543, were recovered in infectious viruses, while all the others were noninfectious constructs. The mutant X515 contains a sequence substitution in a predicted single-stranded loop which may function in either RNA-protein or RNA-RNA interactions. This lesion appeared to affect the in vivo function of poliovirus RNA in the absence of any obvious secondary-structure disruptions. To determine whether the defects caused by the sequence substitutions resulted from a decrease in the efficiency of translation initiation, we carried out in vitro translations of synthetic RNAs harboring the individual linker scanning mutations. We established a strong correlation between the in vivo infectivity of a particular mutant RNA and the level of in vitro protein synthesis.

For the functions involving stem-loop G, maintenance of the predicted secondary structure is not an essential requirement. A highly conserved octamer sequence containing the cryptic AUG at nt 586 ($AUG_{586}$) is located within this hairpin structure. The sequence of this particular $AUG_{586}$, which is present in a favorable sequence context, has been altered to a UUG in a previous study (38). A virus containing the AUG→UUG alteration which exhibited a small-plaque phenotype and decreased levels of viral RNA and protein synthesis was generated. The results suggested that the A residue of the $AUG_{586}$ was required for maximum levels of poliovirus translation but that the $AUG_{586}$ itself was not used for initiation of viral protein synthesis. Three of the linker scanning mutations substitute sequences in stem-loop G, namely, X564, X585, and X607. The mutation X564 replaces sequences of the 3′ half of a conserved polypyrimidine tract present at nt 558. This lesion does not appear to have an effect on viral functions. The linker scanning mutations X585 and X607 substitute sequences on opposite sides of a base-paired stem region. Interestingly, X585 produced a noninfectious construct, while synthetic RNAs containing the X607 mutation yield infectious virus with a wild-type phenotype. These data suggest that the partial destabilization of the hairpin in stem-loop G is not solely responsible for the resulting viral defects. Evidence has been generated in vitro for poliovirus type 2 (Lansing) that supports our observation that base pairing of the stem-loop G can be perturbed without resulting in a decrease in translation initiation. However, if the conserved $AUG_{586}$ was altered at any position, translation initiation was severely impaired. Compensatory mutations on the opposite side of the stem which permitted base pairing with the mutated AUG sequences did not restore translational activity (31).

As further confirmation of the conclusion described above, two virus revertants which contained gross deletions of stem-loop G were isolated upon transfection of HeLa cells with RNAs containing the X585 lesion. No severe defects in viral functions seemed to result from the loss of stem-loop G, suggesting either that this structure does not provide a binding site for protein(s) involved in viral translation (or other viral functions) or that it was not the structure itself that was crucial but rather the distance between stem-loop G and another structure or sequence motif. A third possibility would be that another binding site is formed or uncovered through the deletion. No significant structure is predicted to form in the revertant Se1-5NC-X585$\Delta_1$, according to a computer-based RNA FOLD program. It should be noted that mutants containing deletions with boundaries very similar to those of X585$\Delta_1$ were constructed by site-specific deletion mutagenesis of cDNAs corresponding to the type 1 (Mahoney) strain of poliovirus (employed in the present study) and the Sabin type 1 vaccine strain (12). The Mahoney strain deletion mutant [called PV1(M)IC-DA21] had growth properties similar to those of wild-type virus, in agreement with our results for the Se1-5NC-X585$\Delta_1$ virus.

The Sabin strain deletion mutant [called PV1(Sab)IC-DA21] was impaired for growth and produced reduced levels of virus-specific proteins in infected cells compared with those of cells infected with the Sabin 1 parent virus. Interestingly, both mutant viruses had reduced lesion scores compared with their respective parental viruses, when analyzed by a monkey neurovirulence test. Recently, experimental evidence which demonstrated that stem-loop G is not required for in vitro translation of type 2 poliovirus RNA has been produced (31).

The RNA electrophoretic mobility shift analysis revealed that a cytoplasmic factor(s) does not bind RNA derived from the X585 mutant but that binding is restored in the deletion mutant, X585R. This result is confirmed by the direct binding of factors present in HeLa B-cut extracts to RNAs containing the X585R lesion. The linker-substituted sequences of X585 perturb binding of the protein(s) either because of either the altered primary sequence or because of the destabilized secondary structure. It was surprising that RNA containing the X607 lesion does not bind the factor(s). How can RNA containing the X607 mutation produce a virus with a wild-type phenotype? Perhaps a second-site reversion occurred at a distal location in the viral RNA genome which compensates for this mutation. Formally, such a possibility exists, since only ~100 nt surrounding the *Xho*I linker substitution site in RNA recovered from mutant virus Sel-5NC-X607 were sequenced. However, the lesion of X607 was reconstructed by PCR and reintroduced into a wild-type cDNA of PV1. RNA transfection of the mutant RNAs of X607R in HeLa cells resulted in a virus with a phenotype very similar to that of Sel-5NC-X607 (data not shown). Thus, compensatory mutations are probably not responsible for the translation properties of the mutant. It is clear that for the two mutations described in this study (X585 and X607), alteration of the stem structure in stem-loop G reduces or eliminates the RNA-protein interaction shown in Fig. 7. However, binding of the protein to the sequences in stem-loop G does not appear to be essential for infectivity. The functional role of this interaction remains undetermined.

Other investigators have suggested that the translational efficiency of picornaviruses depends on the proper spacing between two motifs in the 5′ NCR: the polypyrimidine tract at nt 558 and the cryptic $AUG_{586}$ (16, 44). The distance between these two motifs is 22 nt in the 5′ NCR of wild-type poliovirus RNA. A change of this distance would be predicted to cause a decrease in translational efficiency of the viral RNA template. We observed that alteration of one of these motifs, i.e., the $AUG_{586}$ in the mutant X585, dramatically reduces translation efficiency in vitro. The isolated revertant Sel-5NC-X585$\Delta_1$ exhibits a gross deletion which removes not only the altered $AUG_{586}$ but the entire stem-loop G. This deletion regenerates a similar distance of 29 nt between the polypyrimidine tract and an $AUG_{743}$, the authentic translation start site. In the second X585 revertant, Sel-5NC-X585$\Delta_2$, the deletion of stem-loop G and adjacent sequences results in a spacing of 23 nt between the conserved pyrimidine-rich tract and the $AUG_{743}$. The proper distance between these two motifs may permit the factor(s) to bind and mediate internal translation initiation. It remains to be determined whether such a factor is indeed the p52 protein described by Meerovitch et al. (32). Similar distance requirements may also contribute to the initiation process for related viral and cellular mRNAs which utilize cap-independent translation initiation. A factor(s) involved in such internal translation initiation processes that is capable of recognizing two different sequence-specific elements (C- and U-rich region and AUGs) separated by a proper distance must be produced by the host cell. It would not be surprising if this factor(s) or a related protein(s) interacts with cellular mRNAs, like those encoding Bip (28), which are capable of initiating translation following internal binding of ribosomes.

Collectively, our data establish at least two different modes by which stem-loop structures direct translation initiation from the 5′ NCR of poliovirus. The preserved stem-loop F appears to be absolutely required for both virus infectivity and translation initiation. Moreover, this stem-loop must be properly base paired for optimal function and/or activity, since mutations that lead to destabilization of stem sequences abolish or dramatically reduce translation initiation. In contrast, although there is some required structural component in the function of stem-loop G, its primary role may be to provide an AUG codon properly spaced downstream from the polypyrimidine tract. Recognition of the polypyrimidine tract properly spaced from the $AUG_{586}$ may provide a nucleation site for the final assembly of a translation initiation complex. Once assembled, the complex may actually scan the RNA until it encounters the next AUG, as has been suggested by Jackson and colleagues for EMCV (13). None of the enterovirus genomic RNAs contain AUG sequences between the $AUG_{586}$ (or its equivalent) and the start codon at nt 743 (or its equivalent), suggesting that there may be a selection against the presence of AUGs in this region because they would be deleterious to the successful initiation process. In addition, Kuge and colleagues have shown that insertion of AUG sequences in the equivalent region of the Sabin 1 genome is deleterious to viral functions (22). Indeed, two revertant viruses described in the present report restore near wild-type spacing between the polypyrimidine tract and the $AUG_{743}$ without generating any new AUG sequences and, apparently, without regenerating a stem-loop structure equivalent to the sequences in stem-loop G. Perhaps a universally conserved feature of RNA-protein interactions that affect picornavirus translation initiation is the spacing between specific nucleotide sequence elements (7) that may have primary-sequence and secondary-structure determinants. Unraveling the higher-order structures that result from the RNA-protein and RNA-RNA interactions encoded in the 5′ NCR of picornavirus RNAs may ultimately reveal how internal ribosomal entry sites are utilized in translation initiation for a limited set of cellular mRNAs.

## ACKNOWLEDGMENTS

We thank Stephen Sharp for sharing his expertise on linker scanning mutagenesis and Sandra Dildine, Wade Blair, and William Charini for critical comments on the manuscript. We also thank Hung Nguyen for expert technical assistance. We thank V. Agol for communication of data prior to publication.

This work was supported by Public Health Service grant AI26765 and by core support from the Irvine Research Unit in Animal Virology (University of California, Irvine, Calif.). A.A.H. is supported by a predoctoral fellowship from the University of California Biotechnology Research and Education Program.

## REFERENCES

1. **Belsham, G. J., and J. K. Brangwyn.** 1990. A region of the 5′ noncoding region of foot-and-mouth disease virus RNA directs efficient internal initiation of protein synthesis within cells: involvement with the role of L protease in translational control. J. Virol. **64**:5389–5395.
2. **Bienkowska-Szewczyk, K., and E. Ehrenfeld.** 1988. An internal 5′-noncoding region required for translation of poliovirus RNA in vitro. J. Virol. **62**:3068–3072.
3. **Blair, W. S., S.-S. Hwang, M. F. Ypma-Wong, and B. L. Semler.**

1990. A mutant poliovirus containing a novel proteolytic cleavage site in VP3 is altered in viral maturation. J. Virol. **64**:1784–1793.

4. **Brown, B. A., and E. Ehrenfeld.** 1979. Translation of poliovirus RNA *in vitro*: changes in cleavage pattern and initiation sites by ribosomal salt wash. Virology **97**:396–405.
5. **Campos, R., and L. P. Villarreal.** 1982. An SV40 deletion mutant accumulates late transcripts in a paranuclear extract. Virology **119**:1–11.
6. **Dildine, S. L., and B. L. Semler.** 1992. Conservation of RNA-protein interactions among picornaviruses. J. Virol. **66**:4364–4376.
7. **Dildine, S. L., K. R. Stark, A. A. Haller, and B. L. Semler.** 1991. Poliovirus translation initiation: differential effects of directed and selected mutations in the 5′ noncoding region of viral RNAs. Virology **182**:742–752.
8. **Evans, D. M. A., G. Dunn, P. D. Minor, G. C. Schild, A. J. Cann, G. Stanway, J. W. Almond, K. Currey, and J. V. Maizel.** 1985. Increased neurovirulence associated with a single nucleotide change in a noncoding region of the Sabin type 3 poliovaccine genome. Nature (London) **314**:548–550.
9. **Garcia, A. D., A. M. O'Connell, and S. J. Sharp.** 1987. Formation of an active transcription complex in the *Drosophila melanogaster* 5S RNA gene is dependent on an upstream region. Mol. Cell. Biol. **7**:2046–2051.
10. **Hamlyn, D. H., G. G. Brownlee, C. C. Cheng, M. J. Gait, and C. Milstein.** 1978. Complete sequence of constant 3′ noncoding regions on an immunoglobulin mRNA using the dideoxy nucleotide method of RNA sequencing. Cell **15**:1067–1075.
11. **Helentjaris, T., E. Ehrenfeld, M. L. Brown-Luedi, and J. W. B. Hershey.** 1979. Alteration in initiation factor activity from poliovirus-infected HeLa cells. J. Biol. Chem. **254**:10973–10978.
12. **Iizuka, N., M. Kohara, K. Hagino-Yamagishi, S. Abe, T. Komatsu, K. Tago, M. Arita, and A. Nomoto.** 1989. Construction of less neurovirulent polioviruses by introducing deletions into the 5′ noncoding sequence of the genome. J. Virol. **63**:5354–5363.
13. **Jackson, R. J., M. T. Howell, and A. Kaminski.** 1990. The novel mechanism of initiation of picornavirus RNA translation. Trends Biochem. Sci. **15**:477–483.
14. **Jang, S. K., M. V. Davies, R. J. Kaufman, and E. Wimmer.** 1989. Initiation of protein synthesis by internal entry of ribosomes into the 5′ nontranslated region of encephalomyocarditis virus RNA in vivo. J. Virol. **63**:1651–1660.
15. **Jang, S. K., H. G. Kräusslich, M. J. H. Nicklin, G. M. Duke, A. C. Palmenberg, and E. Wimmer.** 1988. A segment of the 5′ untranslated region of encephalomyelitis virus RNA directs internal entry of ribosomes during in vitro translation. J. Virol. **62**:2636–2643.
16. **Jang, S. K., T. V. Pestova, C. U. T. Hellen, G. W. Witherell, and E. Wimmer.** 1990. Cap-independent translation of picornavirus RNAs: structure and function of the internal ribosomal entry site. Enzyme **44**:292–309.
17. **Jang, S. K., and E. Wimmer.** 1990. Cap-independent translation of encephalomyocarditis virus RNA: structural elements of the internal ribosomal entry site and involvement of a cellular 57-kD RNA-binding protein. Genes Dev. **4**:1560–1572.
18. **Kaminski, A., T. Howell, and R. J. Jackson.** 1990. Initiation of encephalomyocarditis virus RNA translation: the authentic initiation site is not selected by a scanning mechanism. EMBO J. **9**:3753–3759.
19. **Kawasaki, E.** 1990. Amplification of RNA, p. 21–27. *In* M. A. Innis, D. H. Gelfand, J. J. Sninsky, and T. J. White (ed.), PCR protocols. A guide to methods and applications. Academic Press, Inc., San Diego, Calif.
20. **Konarska, M. M., and P. A. Sharp.** 1986. Electrophoretic separation of complexes involved in the splicing of precursors to mRNAs. Cell **46**:845–855.
21. **Kozak, M.** 1989. The scanning model for translation: an update. J. Cell Biol. **108**:229–241.
22. **Kuge, S., N. Kawamura, and A. Nomoto.** 1989. Genetic variation occuring in the genome of an in vitro insertion mutant of poliovirus type 1. J. Virol. **63**:1069–1075.
23. **Kühn, R., N. Luz, and E. Beck.** 1990. Functional analysis of the internal translation initiation site of foot-and-mouth disease virus. J. Virol. **64**:4625–4631.
24. **Kuhn, R. J., E. Wimmer, and B. L. Semler.** 1987. Expression of the poliovirus genome from infectious cDNA is dependent upon arrangement of eukaryotic and prokaryotic sequences in recombinant plasmids. Virology **157**:560–564.
25. **Laemmli, U. K.** 1970. Cleavage of structural proteins during the assembly of the head of bacteriophage T4. Nature (London) **227**:680–685.
26. **LaMonica, N., C. Meriam, and V. R. Racaniello.** 1986. Mapping of sequences required for mouse neurovirulence of poliovirus type 2 Lansing. J. Virol. **57**:515–525.
27. **Lawson, M. A., B. Dasmahapatra, and B. L. Semler.** 1990. Species-specific substrate interactions of picornavirus 3C proteinase suballelic exchange mutants. J. Biol. Chem. **265**:15920–15931.
28. **Macejak, D. G., and P. Sarnow.** 1991. Internal initiation of translation mediated by the 5′ leader of a cellular mRNA. Nature (London) **353**:90–94.
29. **Manzella, J. M., and P. J. Blackshear.** 1990. Regulation of rat ornithine decarboxylase mRNA translation by its 5′-untranslated region. J. Biol. Chem. **265**:11817–11822.
30. **McKnight, S. L., and R. Kingsbury.** 1982. Transcriptional control signals of a eukaryotic protein-coding gene. Science **217**:316–324.
31. **Meerovitch, K., R. Nicholson, and N. Sonenberg.** 1991. In vitro mutational analysis of *cis*-acting RNA translational elements within the poliovirus type 2 5′ untranslated region. J. Virol. **65**:5895–5901.
32. **Meerovitch, K., J. Pelletier, and N. Sonenberg.** 1989. A cellular protein that binds to the 5′-noncoding region of poliovirus RNA: implications for internal translation initiation. Genes Dev. **3**:1026–1034.
33. **Minor, P. D., and G. Dunn.** 1988. The effect of sequences in the 5′ non-coding region on the replication of polioviruses in the human gut. J. Gen. Virol. **69**:1091–1096.
34. **Muller, A. J., and O. N. Witte.** 1989. The 5′ noncoding region of the human leukemia-associated oncogene *BCR/ABL* is a potent inhibitor of in vitro translation. Mol. Cell. Biol. **9**:5234–5238.
35. **Najita, L., and P. Sarnow.** 1990. Oxidation-reduction sensitive interaction of a cellular 50-kDa protein with an RNA hairpin in the 5′ noncoding region of the poliovirus genome. Proc. Natl. Acad. Sci. USA **87**:5846–5850.
36. **Nicholson, R., J. Pelletier, S. Le, and N. Sonenberg.** 1991. Structural and functional analysis of the ribosome landing pad of poliovirus type 2: in vivo translational studies. J. Virol. **65**:5886–5894.
37. **Nomoto, A., B. Detjen, R. Pozzatti, and E. Wimmer.** 1977. The location of the polio genome protein in viral RNAs and its implication for RNA synthesis. Nature (London) **268**:208–213.
38. **Pelletier, J., M. E. Flynn, G. Kaplan, V. Racaniello, and N. Sonenberg.** 1988. Mutational analysis of upstream AUG codons of poliovirus RNA. J. Virol. **62**:4486–4492.
39. **Pelletier, J., G. Kaplan, V. R. Racaniello, and N. Sonenberg.** 1988. Cap-independent translation of poliovirus mRNA is conferred by sequence elements within the 5′ noncoding region. Mol. Cell. Biol. **8**:1103–1112.
40. **Pelletier, J., and N. Sonenberg.** 1985. Insertion mutagenesis to increase secondary structure within the 5′ noncoding region of a eukaryotic mRNA reduces translational efficiency. Cell **40**:515–526.
41. **Pelletier, J., and N. Sonenberg.** 1988. Internal initiation of translation of eukaryotic mRNA directed by a sequence derived from poliovirus RNA. Nature (London) **334**:320–325.
42. **Pestova, T. V., C. U. T. Hellen, and E. Wimmer.** 1991. Translation of poliovirus RNA: role of an essential *cis*-acting oligopyrimidine element within the 5′ nontranslated region and involvement of a cellular 57-kilodalton protein. J. Virol. **65**:6194–6204.
43. **Pilipenko, E. V., V. M. Blinov, L. I. Romanova, A. N. Sinyakov, S. V. Maslova, and V. I. Agol.** 1989. Conserved structural domains in the 5′-untranslated region of picornaviral genomes: an analysis of the segment controlling translation and neurovirulence. Virology **168**:201–209.

44. **Pilipenko, E. V., A. P. Gmyl, S. V. Maslova, Y. V. Svitkin, A. N. Sinyakov, and V. I. Agol.** 1992. Prokaryotic-like cis-elements in the cap-independent internal initiation of translation on picornavirus RNA. Cell **68:**119–131.
45. **Sanger, F., S. Nicklen, and A. R. Coulson.** 1977. DNA sequencing with chain-terminating inhibitors. Proc. Natl. Acad. Sci. USA **74:**5463–5467.
46. **Skinner, M. A., V. R. Racaniello, G. Dunn, J. Cooper, P. D. Minor, and J. W. Almond.** 1989. New model for the secondary structure of the 5′ non-coding RNA of poliovirus is supported by biochemical and genetic data that also show that RNA secondary structure is important in neurovirulence. J. Mol. Biol. **207:**379–392.
47. **Vaheri, A., and J. S. Pagano.** 1965. Infectious poliovirus RNA: a sensitive method of assay. Virology **27:**435–436.
48. **Ypma-Wong, M. F., and B. L. Semler.** 1987. *In vitro* molecular genetics as a tool for determining the differential cleavage specificities of the poliovirus 3C proteinase. Nucleic Acids Res. **15:**2069–2088.